Limnol. Oceanogr., 43(5), 1998, 982–986

Ocean scalar irradiance near-surface maxima

Abstract—Estimates of the in-water spectral scalar irradiance, E_0, are needed to quantify the photosynthetically available radiation. When a highly scattering, optically thick medium is illuminated at its surface, it is possible under certain conditions for E_0 to increase with penetration depth near the surface, even if there are no internal sources at the wavelength of interest. Analysis and numerical examples presented here help to explain and quantify the magnitude and location of potential subsurface E_0 peaks in source-free ocean waters and the dependence of the phenomenon on the seawater optical properties and surface conditions. Peaking in E_0 most likely occurs when the incident illumination is strongly directed at the zenith angle, and the location of the maximum is deepest when the asymmetry of the scattering phase function is large. The presence of surface waves and internal reflection greatly reduces the chance of E_0 peaks being present, making a maximum in E_0 below the surface possible only if the single scattering albedo, ω_0, is >0.95 in homogeneous waters or at potentially smaller values if ω_0 increases with depth.

In optical oceanography it is generally assumed that the in situ scalar irradiance $E_0(\tau)$ decreases monotonically with optical depth τ. Although it is well known that the radiance in a particular direction can increase with depth near the surface (Preisendorfer 1976; Mobley 1994), it is generally assumed that in the absence of internal sources the various direction-integrated irradiances decrease from the surface in an approximately exponential manner (e.g. Kirk 1994*b*). In contrast, researchers studying optics in biological tissue have reported $E_0(\tau)$ profiles that increase with penetration depth near the surface and reach a peak before dropping off monotonically. Scalar irradiance peaking has been both predicted by theoretical models (e.g. Flock et al. 1989; Jacques and Prahl 1987; Rastegar et al. 1989; Star et al. 1988) and observed in experimental measurements on tissue phantoms (Moes et al. 1989; Star et al. 1987). Analogously, Lassen et al. (1992) observed a peak in the infrared and near-infrared scalar irradiance in marine microbial mats, and Sanchez (pers. comm.) has reported computing peaks in nuclear reactor neutronic fluxes.

It is important to know if and where $E_0(\tau)$ peaking can occur in natural waters in order to accurately estimate from surface measurements the total photosynthetically available radiation (PAR) for randomly oriented phytoplankton in ocean water or for algal mats at the bottom of ice layers. We investigate both analytically and with numerical simulations the cause of $E_0(\tau)$ peaking and predict under what conditions this phenomenon might be observed in natural waters. The location and magnitude of $E_0(\tau)$ maximums are determined by solving the classical albedo problem of radiative transfer theory for particular seawater properties and surface illumination conditions.

Analysis—We are interested in the radiance L that satisfies the integrodifferential radiative transfer equation

$$\mu\partial L(\tau, \mu)/\partial\tau + L(\tau, \mu) = \omega_0(\tau)\int_{-1}^{1}\tilde{\beta}(\tau, \mu'\rightarrow\mu)L(\tau, \mu')\mathrm{d}\mu', \quad (1)$$

where τ is the dimensionless downward optical depth measured from the surface and the single-scattering albedo, ω_0, is the ratio of spectral volume scattering coefficient b to the spectral volume attenuation coefficient c, with $\omega_0 \leq 1$. Here $L(\tau, \mu)$ is the spectral radiance, integrated over the azimuthal angle, whose direction cosine with respect to τ is μ, and $\tilde{\beta}$ is the azimuthally integrated spectral scattering phase function. Internal sources, such as from fluorescence, bioluminescence, or Raman scattering, are not considered here.

The scalar irradiance $E_0(\tau) = E_{0d}(\tau) + E_{0u}(\tau)$ is given in terms of its downward and upward components by

$$E_{0d}(\tau) = \int_0^1 L(\tau, \mu)\,\mathrm{d}\mu \text{ and } E_{0u}(\tau) = \int_{-1}^0 L(\tau, \mu)\,\mathrm{d}\mu, \quad (2)$$

and the irradiance $E(\tau) = E_d(\tau) - E_u(\tau)$ is given by

$$E_d(\tau) = \int_0^1 \mu L(\tau, \mu)\, d\mu \quad \text{and} \quad E_u(\tau) = \int_{-1}^0 |\mu| L(\tau, \mu)\, d\mu. \tag{3}$$

The ratio $\bar{\mu}(\tau) = E(\tau)/E_0(\tau)$ is the mean cosine of the radiance distribution.

Scalar irradiance peaking can occur when the surface illumination is highly directed in the vertical direction and the ratio of scattering to absorption is high. An increase of photon density with depth occurs due to the decrease with depth of the average vertical component of the velocity of the photons. This vertical velocity at a given depth is $\bar{\mu}(\tau)\tilde{c}$, where $\tilde{c}$ is the speed of light at the wavelength of interest. As $\bar{\mu}(\tau)$ decreases with depth near the surface, the downward vertical progress of the photons slows, and, if absorption is low, the concentration of photons increases. Consider the idealized case where highly collimated light is incident at the surface of a nonabsorbing medium. If the scattering of the incident light is predominantly into directions in the downward hemisphere so that scattering into upward directions can be ignored to first order, then for some depth τ_1, $E(\tau_1) \approx E_d(0^+)$, the downward irradiance just below the surface, and thus $E_0(\tau_1) = E(\tau_1)/\bar{\mu}(\tau_1) \approx \bar{\mu}(0^+)E_0(0^+)/\bar{\mu}(\tau_1)$. Therefore, $E_0(\tau_1) > E_0(0^+)$, provided that $\bar{\mu}(0^+) > \bar{\mu}(\tau_1)$. For this special (unrealistic) example, the magnitude of the irradiance peak could be near a factor of 2 greater than $E_0(0^+)$ as $\bar{\mu}(\tau)$ decreases from near unity at the surface to near 0.5 at large depths. However, in realistic cases, the presence of absorption and scattering into $E_u(\tau)$ tends to cause $E(\tau)$ to decrease with depth, thus reducing the likelihood and magnitude of a $E_0(\tau)$ peak.

To see how absorption and backscattering affect $E_0(\tau)$ profiles, consider a homogeneous, semi-infinite body of water with a purely collimated incident illumination at an assumed flat surface with boundary conditions

$$L(0, \mu) = \delta(\mu - \mu_0)/\mu_0, \qquad 0 \le \mu \le 1, \tag{4}$$

$$L(\infty, \mu) = 0, \qquad \mu < 0, \tag{5}$$

and let us here ignore the index of refraction mismatch. A single-scattering approximation allows us to write (Gordon 1994)

$$L(\tau, \mu) \approx L^{(0)}(\tau, \mu) + \omega_0 L^{(1)}(\tau, \mu) + O(\omega_0^2), \tag{6}$$

where the unscattered light is given by

$$L^{(0)}(\tau, \mu) = \begin{cases} \exp(-\tau/\mu)\delta(\mu - \mu_0)/\mu_0, & \mu \ge 0 \\ 0, & \mu < 0 \end{cases} \tag{7}$$

and $L^{(1)}(\tau, \mu)$ is light that has been scattered only once. The governing equations for $L^{(1)}(\tau, \mu)$ are obtained by inserting Eq. 6 into Eq. 1, 4, and 5 and extracting the terms containing ω_0 to the first power,

$$\mu \frac{\partial L^{(1)}(\tau, \mu)}{\partial \tau} + L^{(1)}(\tau, \mu) = \tilde{\beta}(\mu_0 \to \mu)\exp(-\tau/\mu_0)/\mu_0, \tag{8}$$

$$L^{(1)}(0, \mu) = L^{(1)}(\infty, -\mu) = 0, \qquad \mu \ge 0, \tag{9}$$

which have the solution

$$L^{(1)}(\tau, \mu) = \tilde{\beta}(\mu_0 \to \mu)\frac{\exp(-\tau/\mu_0) - \exp(-\tau/\mu)}{\mu_0 - \mu}, \quad \mu > 0, \tag{10}$$

$$L^{(1)}(\tau, \mu) = \tilde{\beta}(\mu_0 \to \mu)\frac{\exp(-\tau/\mu_0)}{\mu_0 - \mu}, \qquad \mu \le 0. \tag{11}$$

Eq. 10 and 11 are consistent with the leading-order terms in Eq. 4 and 5 of Pahor (1968). The single-scattering approximations to the downward and upward scalar irradiances are

$$E_{0d}(\tau) \approx \exp(-\tau/\mu_0) + \omega_0 \int_0^1 \tilde{\beta}(\mu_0 \to \mu)\frac{\exp(-\tau/\mu_0) - \exp(-\tau/\mu)}{\mu_0 - \mu}\, d\mu, \tag{12}$$

$$E_{0u}(\tau) \approx \omega_0 \exp(-\tau/\mu_0) \int_{-1}^0 \frac{\tilde{\beta}(\mu_0 \to \mu)}{\mu_0 - \mu}\, d\mu. \tag{13}$$

For any $\mu < \mu_0$, the factor $[\exp(-\tau/\mu_0) - \exp(-\tau/\mu)]/(\mu_0 - \mu)$ in the integrand of Eq. 12 exhibits peaking with depth, increasing from zero at the surface to a maximum before decaying exponentially at large depths. The peak magnitude is greatest and shallowest for small μ. For example, for μ of 0.1 the maximum is 0.77 at τ of 0.26, while for μ of 0.9 the maximum is 0.39 at τ of 0.95. Eq. 13 indicates that the single-scattering $E_{0u}(\tau)$ decays monotonically with depth, although peaking in $E_{0u}(\tau)$ can occur once higher order multiple scattering is considered.

Peaking in the single-scattering $E_0(\tau)$, obtained from the summation of Eq. 12 and 13, is most likely and most pronounced if ω_0 is large, giving high weighting to the last term in Eq. 12. Natural waters exhibit a large range of values of ω_0, and ω_0 is sometimes very high near the coast. The peaking is greatest when the amount of backscattering is small, as determined by $\tilde{\beta}(\mu_0 \to \mu)$ for $\mu < 0$, which keeps $E_{0u}(\tau)$ small. For $\mu > 0$, peaking is greatest when the shape of $\tilde{\beta}(\mu_0 \to \mu)$ is such that its magnitude is relatively large near μ of 0 and small near μ of 1. However, in natural waters the magnitude of $\tilde{\beta}(\mu_0 \to \mu)$ is always significantly greater near μ of 1 than near μ of 0, more so than of the media studied in the references cited earlier, so we expect that the peaking in ocean waters may be less pronounced than in other media.

Single-scattering analysis, however, does not fully describe the peaking phenomenon. A more rigorous investigation into E_0 peaking can be made by considering the various diffuse attenuation coefficients. Differentiation of the relationship $\bar{\mu}(\tau) = E(\tau)/E_0(\tau)$ gives

$$K_{\bar{\mu}} = K_E - K_0, \tag{14}$$

where $K_{\bar{\mu}} = -(c/\bar{\mu})(d\bar{\mu}/d\tau)$, $K_E = -(c/E)(dE/d\tau)$, and $K_0 = -(c/E_0)(dE_0/d\tau)$. Peaking in E_0 can only occur if $K_0 < 0$ ($dE_0/d\tau > 0$) between the surface and the depth of maximum E_0. Because K_E in source-free waters is always positive (Mobley 1994, p. 281), it follows from Eq. 14 that K_0 is negative if

$$K_{\bar{\mu}} > K_E. \tag{15}$$

This requires that $d\bar{\mu}/d\tau$ be negative, which is typically the case just below the surface, with $\bar{\mu}(\tau)$ either decreasing monotonically with depth or reaching a minimum before increasing toward an asymptotic value (Bannister 1992); equations are available for predicting which case will occur (McCormick 1995). The magnitude of $|d\bar{\mu}/d\tau|$ near the surface is largest and that of $|dE/d\tau|$ is smallest when ω_0 is large (Berwald et al. 1995). Therefore, Eq. 15 is most likely to be satisfied when ω_0 is large and when the sun is at the zenith, the sky is clear, and the sea state is calm so that $\bar{\mu}$ is near unity.

Another way to view the question of peaking is to use an equation (Gershun 1939) for the spectral beam absorption coefficient, $a = \bar{\mu}K_E$. Differentiation of this equation shows that (Zaneveld 1989)

$$K_{\bar{\mu}} = K_a - K_K, \tag{16}$$

where $K_a = -(c/a)(da/d\tau)$ and $K_K = -(c/K_E)(dK_E/d\tau)$. Substitution of this into Eq. 15 gives a second interpretation for peaking,

$$K_a > K_E + K_K. \tag{17}$$

This indicates that E_0 peaking is enhanced when the value of a decreases with depth and is reduced when a increases with depth. This is a multiple-scattering effect due to the increase with depth of the reflectance of the total water volume below. In locally homogeneous waters, Eq. 17 reduces to $-K_K > K_E$.

Numerical simulations—Numerical simulations help to quantify the influence of water properties and surface conditions on the magnitude and location of possible peaks in $E_0(\tau)$. Simulations for inhomogeneous water properties were performed using a Monte Carlo code provided by Gordon (pers. comm.). Simulations for locally homogeneous waters were performed using the discrete-ordinates code DISORTB (Jin and Stamnes 1994) in which the integral in Eq. 1 is approximated by a Guassian quadrature summation and the index of refraction $n = 1.34$ of the water is taken into account by using a discontinuity at the surface in the number of radiative streams. A comparison of the Monte Carlo and DISORTB codes has been given in Mobley et al. (1993). Unless otherwise noted, the boundary condition just above the surface is that of Eq. 4 with $\mu_0 = 1$. The optical depth was 50 and the bottom was purely absorbing.

The simulations showed that internal reflection at the surface, arising from the index of refraction mismatch, has a profound effect on the shape of irradiance profiles. For example, Fig. 1 shows the profile of simulated $E_0(\tau)$ in homogeneous waters. The Petzold particle phase function (Mobley et al. 1993) was used and $\omega_0 = 0.99$. Also shown are the portion of $E_0(\tau)$ due to internal reflection and the portion resulting from photons not internally reflected. It can be seen that if it were not for the index of refraction mismatch at the surface, $E_0(\tau)$ would have a maximum value at τ of 5 that is 32% greater than $E_0(0^+)$ just below the surface. However, the portion of $E_0(\tau)$ due to internal reflection is monotonically decreasing, and the superposition of the two portions of the light field results in an overall $E_0(\tau)$ that in this case peaks by only 1.2%. Therefore, despite the very large peaks in $E_0(\tau)$ predicted when internal reflection is neglected and reported (e.g. in Star et al. 1987), the influence of internal reflection on the light field in the atmosphere–ocean system dominates over the processes that leads to peaking, forcing the magnitude of peaks in $E_0(\tau)$ to be small.

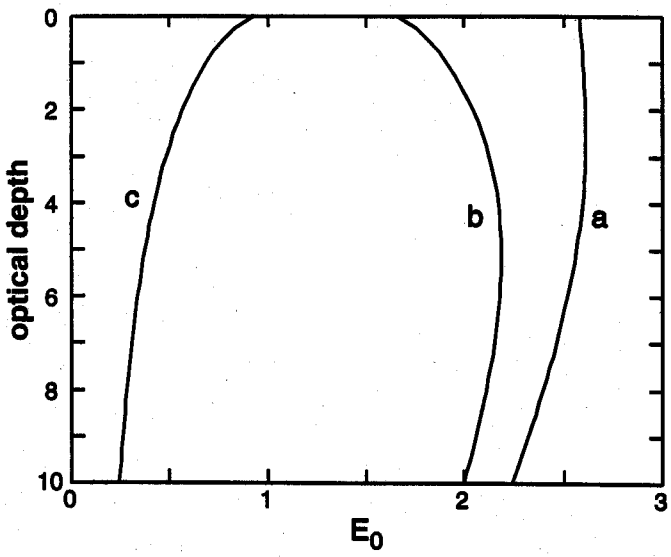

Fig. 1. Scalar irradiance vs. optical depth for the Petzold particle phase function and $\omega_0 = 0.99$. Shown are (a) total $E_0(\tau)$, (b) the portion of $E_0(\tau)$ independent of internal reflection, and (c) the portion due to internal reflection.

Simulations were performed for various values of ω_0 and $\tilde{\beta}$ to determine the effect of the water properties on the magnitude and depth of the $E_0(\tau)$ maximum. The simulations were computed with the Petzold particle phase function and with the Henyey–Greenstein (1941) phase function, which depends on only the scattering asymmetry factor g ($-1 \leq g \leq 1$) that is the mean cosine of the scattering angle for the phase function. In typical ocean waters $0.75 \leq g \leq 0.95$ (Gordon et al. 1993). Selected $E_0(\tau)$ profiles are shown in Fig. 2. Each profile is normalized to unity just below the surface so that the shapes of the profiles can be compared. A subsurface $E_0(\tau)$ maximum only occurred for very large values of ω_0, i.e. $\omega_0 > 0.95$ for the Henyey-Greenstein phase function and $\omega_0 > 0.97$ for the Petzold phase function. The depth of the peak is deepest for large values of g and for large ω_0, and for the Henyey–Greenstein phase function the relative magnitudes of the $E_0(\tau)$ peaks are greatest for $g \approx 0.9$.

Equation 17 indicates that peaking in $E_0(\tau)$ is enhanced by an absorption coefficient that decreases with depth or, equivalently, a single scattering albedo that increases with depth. Figure 3 shows three simulated $E_0(\tau)$ profiles for g of 0.9 with the Henyey–Greenstein phase function, each normalized to unity at the surface. Two of these are for homogeneous waters with ω_0 of 0.90 and 0.95, respectively, while the third is for a $\omega_0(\tau)$ that increases linearly from ω_0 of 0.90 at τ of 0 to ω_0 of 0.95 at τ of 1.0 and is constant at ω_0 of 0.95 for $\tau > 1.0$. While $E_0(\tau)$ in each homogeneous case decreases monotonically with depth, $E_0(\tau)$ in the nonhomogeneous case peaks at about τ of 0.8, confirming that

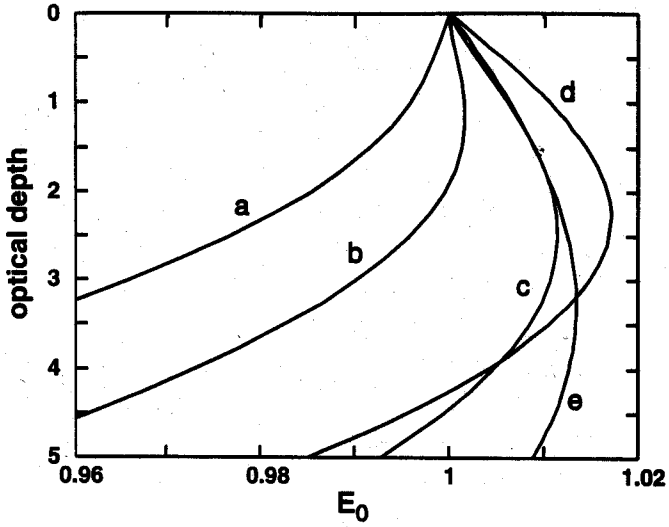

Fig. 2. Scalar irradiance vs. optical depth for locally homogeneous waters. Profiles a, b, and c are for the Petzold particle phase function with $\omega_0 = 0.97$, 0.98, and 0.99, respectively, and cases d and e are for $\omega_0 = 0.99$ and with the Henyey-Greenstein phase function for $g = 0.75$ and 0.95, respectively. Each profile is normalized to its value just beneath the surface, $E_0(0^+) = 1.71$, 1.99, 2.58, 2.20, and 2.86, respectively.

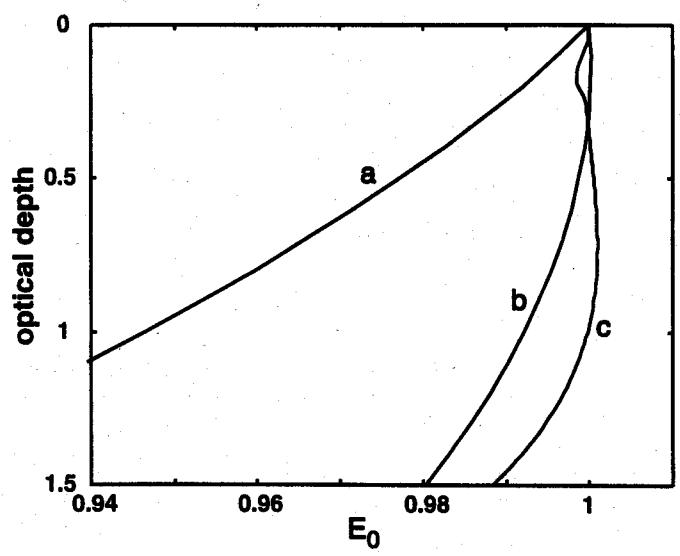

Fig. 3. Scalar irradiance vs. optical depth for $g = 0.9$ and for (a) $\omega_0 = 0.90$, (b) $\omega_0 = 0.95$, and (c) ω_0 increasing linearly from $\omega_0 = 0.90$ at $\tau = 0$ to $\omega_0 = 0.95$ at $\tau = 1.0$, below which ω_0 remains constant. Each profile is normalized to its value just beneath the surface, $E_0(0^+) = 1.28$, 1.58, and 1.53, respectively.

stratification of the water column can enhance, or detract from, the magnitude of a $E_0(\tau)$ peak.

In Figs. 1–3, the illumination used was direct sunlight against a black sky and the sea surface was taken to be flat. Diffuse skylight and surface waves both cause the light field just below the surface to be more diffuse which, as indicated by Eq. 15, reduces the chances of observing an irradiance peak. For example, for ω_0 of 0.99, g of 0.90, the sun at the zenith, and no skylight, there is a 1.6% peak in $E_0(\tau)$, whereas for the same water properties and 75% direct light and 25% skylight, there is only a 0.4% peak in $E_0(\tau)$. Placing the sun at angles other than the zenith also decreases any $E_0(\tau)$ peak. For example, if for these same water properties and no diffuse skylight the sun is moved from the zenith to 8°, the $E_0(\tau)$ peak decreases to 0.38%.

Discussion—Peaking in $E_0(\tau)$ is caused primarily by the portion of the incident radiation at small polar angles that scatters into larger polar angles within the downward hemisphere ($\mu > 0$). This tendency for $E_0(\tau)$ to peak below the surface is greatly dampened by the presence of internal reflection, which adds to the light field a nearly diffuse contribution that is monotoncially decreasing with depth. With internal reflection and a realistic form of the scattering phase function for natural waters, $E_0(\tau)$ peaking can only occur for large values of ω_0. The relative magnitude of $E_0(\tau)$ maxima is greatest for moderately large values of g (~0.9) because backscattering detracts from peaking and because the location of a maximum is deepest for large values of g where the light field is least influenced by internal reflection.

In case 1 waters, ω_0 is typically not large enough for subsurface peaking in $E_0(\tau)$ to occur. It is not surprising that peaking in $E_0(\tau)$ is unlikely in open-ocean waters because it is rarely observed. On the other hand, Kirk (1994*a*) has reported observations of case 2 waters with values of ω_0 as high as 0.994. Also, we note that $E_0(\tau)$ peaking is likely to occur within sea ice, especially for wavelengths near 470 nm where typically $\omega_0 > 0.99$ (Perovich 1996), and should be considered in the modeling of algal mats below sea ice.

R. A. Leathers
N. J. McCormick

Department of Mechanical Engineering
University of Washington
Box 352600
Seattle, Washington 98195-2600

References

BANNISTER, T. T. 1992. Model of the mean cosine of underwater radiance and estimation of underwater scalar irradiance. Limnol. Oceanogr. **374:** 773–780.

BERWALD, J., D. STRAMSKI, C. D. MOBLEY, AND D. A. KIEFER. 1995. Influences of absorption and scattering on vertical changes in the average cosine of the underwater light field. Limnol. Oceanogr. **40:** 1347–1357.

FLOCK, S. T., M. S. PATTERSON, B. C. WILSON, AND D. R. WYMAN. 1989. Monte Carlo modeling of light propagation in highly scattering tissues. IEEE Trans. Biomed. Eng. **36:** 1162–1167.

GERSHUN, A. A. 1939. The light field. J. Math. Phys. [Cambridge, MA] **18:** 51–151.

GORDON, H. R. 1994. Modeling and simulating radiative transfer in

Acknowledgments

This work was supported by grants from the Office of Naval Research and the San Diego Supercomputer Center. We appreciate the use of the DISORTB computer program developed by Zhonghai Jin and the Monte Carlo code developed by Howard Gordon. Niels Højerslev suggested we investigate this problem and provided several insights. We thank the reviewers for their helpful comments.

the ocean, p. 13–15. *In* R. W. Spinrad, K. L. Carder, and M. J. Perry [eds.], Ocean optics. Oxford Univ. Press.

———, K. DING, AND W. GONG. 1993. Radiative transfer in the ocean: Computations relating to the asymptotic and near-asymptotic daylight field. Appl. Opt. **32:** 1606–1619.

HENYEY, L. C., AND J. L. GREENSTEIN. 1941. Diffuse radiation in the galaxy. Astrophys. J. **93:** 70–83.

JACQUES, S. L., AND S. A. PRAHL. 1987. Modeling optical and thermal distributions in tissue during laser irradiation. Lasers Surg. Med. **6:** 494–503.

JIN, Z., AND K. STAMNES. 1994. Radiative transfer in nonuniformly refracting layered media such as the atmosphere/ocean system. Appl. Opt. **33:** 431–442.

KIRK, J. T. O. 1994*a*. Characteristics of the light field in highly turbid waters: A Monte Carlo study. Limnol. Oceanogr. **36:** 702–706.

———. 1994*b*. Light and photosynthesis in aquatic ecosystems, 2nd ed. Cambridge Univ. Press.

LASSEN, C., H. PLOUG, AND B. B. JORGENSEN. 1992. Microalgal photosythesis and spectral scalar irradiance in coastal marine sediments of Limfjorden, Denmark. Limnol. Oceanogr. **37:** 760–772.

MCCORMICK, N. J. 1995. Mathematical models for the mean cosine of irradiance and the diffuse attenuation coefficient. Limnol. Oceanogr. **40:** 1013–1018.

MOBLEY, C. D. 1994. Light and water. Radiative transfer in natural waters. Academic.

———, AND OTHERS. 1993. Comparison of numerical models for computing underwater light fields. Appl. Opt. **32:** 7484–7504.

MOES, C. J. M., M. J. C. VAN GEMERT, W. M. STAR, J. P. A. MARIJNISSEN, AND S.A. PRAHL. 1989. Measurements and calculations of the energy fluence rate in a scattering and absorbing phantom at 633 nm. Appl. Opt. **28:** 2292–2296.

PAHOR, S. 1968. Multiple scattering and the inverse albedo problem. Phys. Rev. **175:** 218–221.

PEROVICH, D. K. 1996. The optical properties of sea ice. U.S. Army Corps of Engineers, Cold Regions Res. & Eng. Lab., Springfield, Virginia.

PREISENDORFER, R. W. 1976. Hydrologic optics. V. 1. NTIS PB 259793/8ST. Natl. Tech. Inform. Serv., Springfield, Virginia.

RASTEGAR, S., M. MOTAMEDI, A. J. WELCH, AND L. HAYES. 1989. A theoretical study of the effect of optical properties in laser ablation of tissue. IEEE Trans. Biomed. Eng. **36:** 1180–1187.

STAR, W. M., H. P. A. MARJINISSEN, H. JANSEN, M. KEIJZER, AND M. J. C. VAN GEMERT. 1987. Light dosimetry for photodynamic therapy by whole bladder wall irradiation. Photochem. Photobiol. **46:** 619–624.

———, AND OTHERS. 1988. Light dosimetry in optical phantoms and in tissues. I. Multiple flux and transport theory. Phys. Med. Biol. **33:** 437–454.

ZANEVELD, J. R. V. 1989. An asymptotic closure theory for irradiance in the sea and its inversion to obtain the inherent optical properties. Limnol. Oceanogr. **34:** 1442–1452.

Received: 16 May 1997
Accepted: 17 November 1997
Amended: 3 December 1997